Title: Drought Induced Snag Dynamics and Fuel Succession in the Sierra Nevada

Author: Hudson Northrop

Highlights:

- Sierra Nevada forests currently contain large pools of combustible biomass in standing dead trees following extensive drought mortality
- As a result of tree mortality, fine woody debris and litter and duff fuel loads increased significantly from 2017 to 2021
- Snag longevity increased with tree size and varied by tree species, with incense-cedar snags standing the longest and yellow pine snags (ponderosa pine and Jeffrey pine) standing the shortest
- Fuel loads are projected to increase sharply in the coming decades as remaining standing dead trees fall to the surface

Abstract:

California recently experienced one of the most severe periods of drought in its recorded history from 2012-2016, which has been followed by widespread tree mortality throughout the state with estimates suggesting over 147 million trees have died. One of the most concerning effects and uncertainties surrounding the episodic mortality is the sudden creation of millions of standing dead trees (snags), sharply increasing snag biomass in Sierra Nevada forests. Despite the importance of snags in influencing wildlife habitat, nutrient cycling, and wildfire effects, the dynamics of snag persistence and decay rates are still not particularly well understood and characterized. Here we attempt to better characterize the likely progression of fuels and snag decay following the recent extensive mortality event in the Sierra Nevada mixed conifer ecosystem using long term annually collected snag demography data and recent surface fuel

measurements from three locations. In the short term (2017-2021) fine woody debris and litter and duff significantly increased across all three study sites, while coarse woody debris increased only at 1one site, and total fuel loads increased at two of the three sites. Across all species snag longevity increased with size with the relationship varying by species. Size played a small role in influencing yellow pine (ponderosa pine and sugar pine) fall rates but a very large role in red fir and sugar pine longevity. Size played an important, but less pronounced role for white fir, incense-cedar, and black oak. Our projections show that the rate of biomass input from future snag fall varies across our three sites and by 2040 we project median cumulative inputs of 136.1 Mg ha^{-1}, 92.3 Mg ha^{-1}, and 49.4 Mg ha^{-1} at each site.

Managers are not without options for how to deal with the extreme number of snags and their large ground combustible biomass. Careful timing and application of prescribed burning and salvage operations may effectively reduce fuel loads and change fuel load trajectories to limit fire risk into the future, but both methods have operational, economic, and legal limitations. This study provides managers with some essential information regarding snag longevity and fuel load accumulation following the extensive drought in the Sierra Nevada that can aid in future decision making.

Keywords: California, snag fall rates, fuel loads, bark beetle mortality, forest management

1. Introduction

California recently experienced one of the most severe periods of drought in its recorded history (Griffin & Anchukaitis, 2014; Robeson, 2015), which has been followed by widespread tree mortality throughout the state with estimates suggesting over 147 million trees have died

47 (USDA 2019). Due to over a century of fire suppression and exclusion without concurrent
48 density management, many Sierra Nevada forests existed at high densities prior to the drought
49 and were likely under much higher competitive stress relative to their pre-European historical
50 conditions (Collins et al., 2011; North et al., 2022). High levels of competition coupled with
51 stress due to five years (2012-2016) of extreme drought limited the ability of trees to resist
52 attacks from insects and pathogens. Ultimately many of these drought-weakened trees died (Kolb
53 et al., 2016; Stephenson et al., 2019). Numerous field-based studies have characterized the
54 immediate impacts of the drought, noting extensive mortality of overstory trees throughout the
55 Sierra Nevada, particularly in the southern region of the range (Axelson et al., 2019; Fettig et al.,
56 2019; Pile et al., 2019). However given that the frequency of droughts of similar magnitudes are
57 projected to increase in the future (Diffenbaugh et al., 2015), it is important to better understand
58 the longer-term impacts of massive tree mortality on forest dynamics. .
59 An immediate concern is that millions of standing dead trees (snags) greatly increase the
60 amount of dead biomass in Sierrian forests. Snags play important roles in many ecosystem
61 processes. They provide important habitat for many cavity-nesting birds and wildlife while
62 standing and can house many invertebrate and fungi species while standing or after falling to the
63 ground (Harmon et al., 1986; Raphael & White, 1984; Saab et al., 2014). The decomposition of
64 snags and the coarse woody debris created when snags fall (CWD) also plays a critical role in the
65 cycling of nutrients and carbon within ecosystems (Cousins et al., 2015; Harmon et al., 1986).
66 Snags also influence wildfire risk and fire behavior. Burning snags can produce embers that
67 facilitate spot fires (Barrows 1951) while decayed snags and coarse woody debris on the ground
68 can provide a receptive surface for spot fires (Knapp, 2015; Stephens, 2004). Furthermore, the
69 combustion of coarse woody material can result in long burnout times that release high amounts

of energy and heat to the soil, increasing severity and effects of fire (Brown et al., 2003; Monsanto & Agee, 2008). More recently, the amount of coarse woody material and density of snags has been associated with high fire severity and mass fires (Jaffe et al., 2021; Lydersen et al., 2019; Stephens et al., 2018).

Despite the importance of snags in influencing wildlife habitat, nutrient cycling, and wildfire effects, the dynamics of snag persistence are not well-characterized, particularly in response to catastrophic mortality events other than wildfire. Studies have identified common traits that influence fall rates, such as size, species, height, and site characteristics (Audley et al., 2021; Parish et al., 2010; Raphael & Morrison, 1987; Rhoades et al., 2020), often reporting that snag longevity varies based on species and that larger trees tend to fall at slower rates. However, many studies focus specifically on trees that were killed by wildfires (Grayson et al., 2022; Ritchie et al., 2013) or report on fall rates in different ecosystems than the Sierra Nevada (Audley et al., 2021; Parish et al., 2010; Rhoades et al., 2020). Despite research on non-fire killed snags in the Sierra Nevada (Raphael & Morrison, 1987), fall rates are rarely studied in a manner that allows managers and scientists to accurately predict the longevity of a given snag. Furthermore, it is not well understood exactly how much dead overstory trees contribute and relate to surface fuel loads over time (Lydersen et al., 2015). With over 147 million dead trees across Sierra Nevada forests, it is essential to understand the potential timing and magnitude of fuel inputs from snags in the coming years as millions of snag decay and fall to the surface.

In the wake of the recent drought-mortality event in the Sierra Nevada, the amount of combustible woody material on the surface floor is expected to dramatically increase as snags decay and fall to the ground, ultimately increasing the potential for mass fires (Stephens et al., 2018). A general model from Hicke et al. (2012) describes multiple phases of fuel and fire risk

93 development following waves of bark beetle mortality, with an initial “red phase” as recently
94 dead canopy fuels dry out and lose moisture, followed by a “gray phase” as fine foliage and
95 branches fall to the ground, shifting fine fuels from the canopy to the surface fuel layer, and then
96 an “old phase” as entire boles and snags fall to the ground, notably increasing surface fuel loads
97 due to an increase of coarse woody debris from fallen snags. It is hypothesized that the Sierra
98 Nevada will follow a similar trend in wake of the recent mortality.
99 A number of studies have observed pulses in fine woody material and litter shortly after
100 bark beetle driven mortality epidemics (Klutsch et al., 2009; Page & Jenkins, 2007; Schoennagel
101 et al., 2012). Similarly, studies have either directly observed large increases in coarse woody
102 material as stands enter the “old phase” (Page & Jenkins, 2007; Schoennagel et al., 2012) or
103 make similar projections of coarse woody debris loads (Collins et al., 2012; Klutsch et al., 2009).
104 While it is generally understood that there should be a contribution to surface fuel loads as snags
105 eventually decay and fall over and deposit woody material to the ground, the exact timing of fall
106 rates and magnitude of fuel inputs are difficult to quantify and vary widely across different
107 ecosystems.
108 Here we attempt to better characterize the likely progression of fuels and snag decay
109 following the recent mortality event in the Sierra Nevada mixed conifer ecosystem. We leverage
110 39 years of annual inventory data and recent surface fuel measurements to quantify short- and
111 long-term trends in surface fuel changes. We also use accelerated failure time models and recent
112 field data to make projections for when snags are likely to fall in the coming decades in
113 Yosemite and Sequoia-Kings Canyon National Parks. The objectives of this study were to 1)
114 determine the short-term changes in fuel loads over the past 5 years in the central and southern
115 Sierra Nevada, 2) develop models describing snag fall rates for common Sierra Nevada species,

and 3) to apply those models to make projections quantifying the magnitude and timing of biomass inputs from snag-fall to surface fuels into the future.

2. Methods

2.1 Study Sites

2.1.1 Site Description for Fuel Load Plots

We sampled fuels data from a network of plots installed in 2017 across the Sierra Nevada to research effects of the 2012-2016 drought mortality (Axelson et al. 2019). For this study, we focus on the three study areas in the Southern Sierra Nevada where drought-induced tree mortality was most extensive (Fettig et al., 2019; Preisler et al., 2017).

The Sequoia-Kings Canyon National Parks (SEKI) site is located in the Crystal Cave area of Sequoia National Park in Tulare County, CA. The 1700-ha study area is managed by the National Park Service and has experienced neither fire nor timber harvests in the last century. Mean elevation is 1687 m. Average annual temperature is 7 °C (January: 0 °C; July: 17 °C) and average annual precipitation is 1143 mm (PRISM Climate Group, 2020). White fir (*Abies concolor,* Gord & Glend) and incense-cedar (*Calocedrus decurrens,* Torr) dominate the site. Although situated near old giant sequoia (*Sequoiadendron giganteum*, Buchholz) groves, no giant sequoia were documented within the study area.

The Yosemite Mixed-Conifer (YOMI) site is situated near the Hodgdon Meadow Campground at the Big Oak Flat Entrance station in Tuolumne County, CA. The 260-ha study site is managed by the National Park Service. Mean elevation is 1422 m. Average annual temperature for the site is 11 °C (January: 4 °C; July: 20 °C) and average annual precipitation is 991 mm (PRISM Climate Group, 2020). The site is dominated by white fir, incense-cedar, and

sugar pine (*Pinus lambertiana,* Dougl.). No recent timber harvests have been conducted at the site. However, prescribed fire was applied across the study area in 2011 and 2012.

The Yosemite Pine (YOPI) site is located along Wawona Rd. 11 km from the southern entrance to Yosemite National Park in Mariposa County, CA. The site spans 397 ha and is managed by the National Park Service. Mean elevation within the site is 1722 m. Average annual temperature is 10 °C (January: 3 °C; July: 19 °C) and average annual precipitation is 1042 mm (PRISM Climate Group, 2020). Ponderosa pine (*Pinus ponderosa* Dougl. Ex Laws), and incense-cedar dominate the site. No recent timber harvests or fires have affected the study site.

2.1.2 Site Description for Snag Fall Rate Modeling Plots

From 1982 to 2001 researchers from the US Geological Survey installed a network of permanent plots ranging from 0.9 ha to 2.5 ha to study forest demography and dynamics in the old-growth mixed conifer forests of Sequoia-Kings Canyon and Yosemite National Parks. For this study, we use a subset of the data in the demography study. The study areas have never been logged and experienced frequent low to moderate severity surface fires prior to Euro-American settlement (Caprio & Swetnam, 1993). Four of our 23 demography plots and portions of the YOMI and SEKI study sites experienced prescribed burns or wildfires in recent decades. The demography plots encompass common mixed-conifer species in the southern Sierra Nevada, such as ponderosa pine, sugar pine, white fir, incense-cedar, Jeffrey pine, red fir (*Abies magnifica,* Pitcher), and black oak (*Quercus kelloggii,* Newb.). The elevations of plots range from 1500 to 2576 m. A portion of the demography plots in Sequoia-Kings Canyon and Yosemite National Parks overlap with the SEKI and YOMI fuel study areas, respectively.

2.2 Field Measurements

2.2.1 Fuels

In 2017, a collection of 29, 35, and 37 circular 0.05-hectare fixed radius plots were established at SEKI, YOMI, and YOPI, respectively. These plots were located randomly using a spatially stratified design (Stevens & Olsen, 2003).When establishing plots in 2017, crews monumented plot centers with a painted rebar stake for later remeasurements. In 2021, field crews located and re-measured all plots established in 2017. Crews recorded the diameter at breast height (height = 1.37m , DBH), species, height, and status (live or dead) of all standing dead trees with a DBH equal to or greater than 10 cm in 2017. Crews also recorded the decay status of snags in 2017, which classifies snag decay based on the condition of the tree's top, branches, twigs, sapwood, and heartwood (USFS, 2010). At each plot fuels were recorded along three transects with azimuths of 90, 210, and 330 degrees following the Brown's fuel protocol (Brown, 1974). Crews tallied 1-hour (<0.64 cm diameter) and 10-hour (0.64-2.54 cm) fuels from 3 to 5 meters along each transect, 100-hour (2.54-7.62 cm) fuels from 3 to 6 meters along each transect. Depths of litter and duff were measured at 3 and 10 m along each transect. Crews measured the diameter and decay status (sound or rotten) of all 1000-hour (>7.62 cm) fuels along the entire length (12.62 m) of each transect. Fuels were measured in both 2017 and 2021.

2.2.2 Snag Fall Rate Data

In the Forest Demography plots (described in 2.1.2 above), all trees taller than 1.37 m in height were tagged, identified to species, measured for diameter, and the location of every tree was mapped. Crews visited plots annually to document tree mortality and status of snags and to tag and measure new (ingrowth) trees. Prior to 2013, crews did not explicitly document when

snags fell over, however, they noted when snags were not found or were found fallen onto the ground. In 2013, researchers combed through the annual plot notes to estimate the year snags fell (Battles. et al., 2015). Beginning in 2013, field crews began explicitly recording the year when snags fell. Snags were considered "fallen" if their main stem, or bole, broke at a height less than or equal to 1.37 m off the ground. We limited our analysis to snags greater than 12.7 cm in DBH.

2.3 Data Analysis

2.3.1 Fuels

We used the RFuels package (Foster et al., 2018) to calculate fuel loads for each fuel category (1-hour, 10-hour, 100-hour, 1000-hour, litter, duff). Transect level estimates were averaged to the plot level, then we used a paired t-test to determine if there were significant differences in fuel loads for each site from 2017 to 2021. The distributions of fuel loads were visually inspected to ensure the assumption of normality for the paired t-tests was met for all fuel categories. Prior to testing for significant differences, we aggregated the fuel calculations into four fuels categories: total fuel loads, fine woody debris fuel loads (1, 10, 100 hour), coarse woody debris fuel loads (1000-hour fuels), and litter and duff fuel loads added together into one category.

2.3.2 Snag Fall Rates

To evaluate snag fall rates, we applied survival analysis that uses the time of occurrence of an event to estimate the probability that the event has occurred by a specific time (Whitlock & Schluter, 2020). A key advantage of survival analysis is that not all subjects in a study need to

experience the event of interest within the time frame of the study. For this study, the event of interest was snag fall, and we were interested in assessing how long snags stood until they fall.

Using the demography dataset, we were able to determine the time each snag was standing. Many of the snags in our dataset had not fallen by the time of the most recent sample and were therefore treated as right-censored.

Some of the demography plots had experienced fire in recent decades. Trees killed by fire often fall at faster rates relative to snags created by other causes (Morrison & Raphael, 1993). Additionally, snags exposed to fire typically experience heightened fall rates compared to unburned snags (Landram et al., 2002). Since we were interested in understanding the fall rates of trees that died from non-fire related causes, we omitted snags created by fire and right-censored pre-existing snags that were exposed to fire. Specifically, we excluded any snags that were created within five years of a fire in our dataset. Research in the Sierra Nevada mixed conifer forests suggest that post-fire mortality levels off by roughly three years post-fire (Hood et al., 2010; Stephens & Finney, 2002). We excluded trees that died up to five years after fire to ensure that snags created afterward likely died from non-fire related causes and therefore would not bias our fall rate estimates. The right-censoring of snags allowed us to extract information about snag persistence from the time those snags were standing prior to the fire, while avoiding the possible confounding effect of fire on the survival rate post-fire.

We quantified the observed snag fall rate for each species using the Kaplan-Meier estimator, a non-parametric technique for estimating and visualizing survival probability over time (Kaplan & Meier, 1958). We also tested for differences in fall rates based on species using the log rank test, which tests the null hypothesis that survival curves for two or more groups are the same (Andersen & Keiding, 2014). We then used accelerated failure time (AFT) models to

project snag survival time. Conceptually, the AFT is a parametric model that defines a baseline survival curve that can include covariates that speed up or slow down the survival times of individuals (James, 2014). We evaluated the fit of five potential underlying distributions that are commonly used when modeling snag fall (Parish et al., 2010; Grayson et al., 2022) rates: Weibull, exponential, lognormal, loglogistic, and gaussian distributions. Based on Akaike Information Criterion (AIC), the loglogistic distribution provided the best underlying fit for the survival curve.

The survival function for the loglogistic distribution is defined by:

$$S(t) = [\,1 + t^{1/\sigma} exp(\tfrac{-\mu - \alpha_i x_i}{\sigma})\,]^{-1} \qquad \text{Equation 1}$$

And the *p*th percentile of the survival distribution for the *i*th individual is $t_i\,(p)$ defined as:

$$t(p) = exp\,[\,\sigma\, log(\tfrac{100-p}{100}) + \mu + \alpha_i x_i\,] \qquad \text{Equation 2}$$

Where:

$$S(t) = probability\ a\ snag\ survives\ to\ a\ given\ time, t$$

$$\sigma = scale\ parameter$$

$$t = time$$

$$\mu = intercept$$

$$\alpha_i x_i = \left(\alpha_1 x_1 + \alpha_2 x_2 + \cdots + \alpha_j x_j\right) where\ \alpha = covariate\ coeficients\ and\ x = covariates$$

We then fit multiple AFT models describing snag fall rates using snag DBH, snag species, and the interaction of snag DBH and species as covariates. Due to small sample size and the difficulty of field crews distinguishing between ponderosa pine and Jeffrey pine in the field, we combined snags of these species into one species category of yellow pine to represent both species. We selected the best model based on lowest AIC score. We assessed the fit of the best

model by comparing binned predicted survival probabilities to observed survival probabilities (Das et al., 2022). To do this, we predicted survival probabilities of each tree using our model, binned results in ten evenly divided classes (i.e., 0.1,0.2,0.3, up to 1.0), and then aggregated adjacent bins until there were at least 50 trees in each bin. We then compared the average predicted survival probability within each bin to the average observed survival probability within each bin. We also assessed model performance by calculating the concordance statistic, which is a measure of how well a model discriminates between dying and surviving objects (where a value of 1 indicates perfect discrimination and a value of 0.5 indicates discrimination that is no better than random). We summarized the effect size of species and DBH by generating predicted survival curves using the best fitting AFT.

2.3.3 Snag fall rate and biomass

Upon determining the best fitting model to describe snag fall rates, we used the 2017 inventory of snags at SEKI, YOMI, and YOPI to forecast the input of biomass to the surface from falling snags at each site. We used regional biomass equations (Forest Inventory and Analysis 2010) to estimate live tree biomass that was originally represented by each snag when it was alive. We then discounted bole biomass in each snag using ratios based on decay class (Cousins et al.2015). Branch biomass in snags was also reduced based on decay class with no degradation in recently dead trees (decay class 1), 0.9 for young snags (decay class 2); 0.4 for middle-aged snags (decay classes 3 and 4), and 0 for old snags (decay class 5). The AFT allowed us to predict the year each snag will fall. Knowing the amount of biomass and expected fall date for each snag, we forecasted snag input to fuel loads at each site.

To characterize the variability and uncertainty associated with our model predictions, we generated forecasts using fall rates in 3 different percentiles, 25th, 50th (median), and 75th percentiles, which correspond to faster or slower overall fall rates. All analyses were conducted in the R statistical software (R Core Team, 2019) and survival modeling utilized the "survival" package in R (Therneau, 2015).

3. Results

3.1 Surface Fuel Load changes

Total fuel loads increased significantly from 2017 to 2021 in SEKI and YOPI with increases of 55.43 Mg ha^{-1} (38.5% increase) and 90.69 Mg ha^{-1} (68.7%) ($p < 0.05$, Supplementary Table S2, Figure 1), respectively but there was no change at YOMI ($p = 0.136$). Fine woody debris fuel loads increased significantly at all 3 sites with average increases of 9.32 (145.2%), 13.32 (189.2%), and 14.17 (148.1%) Mg ha^{-1}, respectively ($p < 0.05$). Coarse woody debris loads did not change significantly at SEKI and YOMI ($p = 0.185$, $p = 0.509$) while loads of coarse woody debris increased significantly by 18.96 Mg ha^{-1} (48.6%) in YOPI ($p = 0.032$). Litter plus duff loads increased significantly at all sites with increases of 48.58 (55.3%), 58.43 (68%), and 50.54 Mg ha^{-1} (101.5%) for SEKI, YOPI, and YOMI, respectively ($p <0.05$).

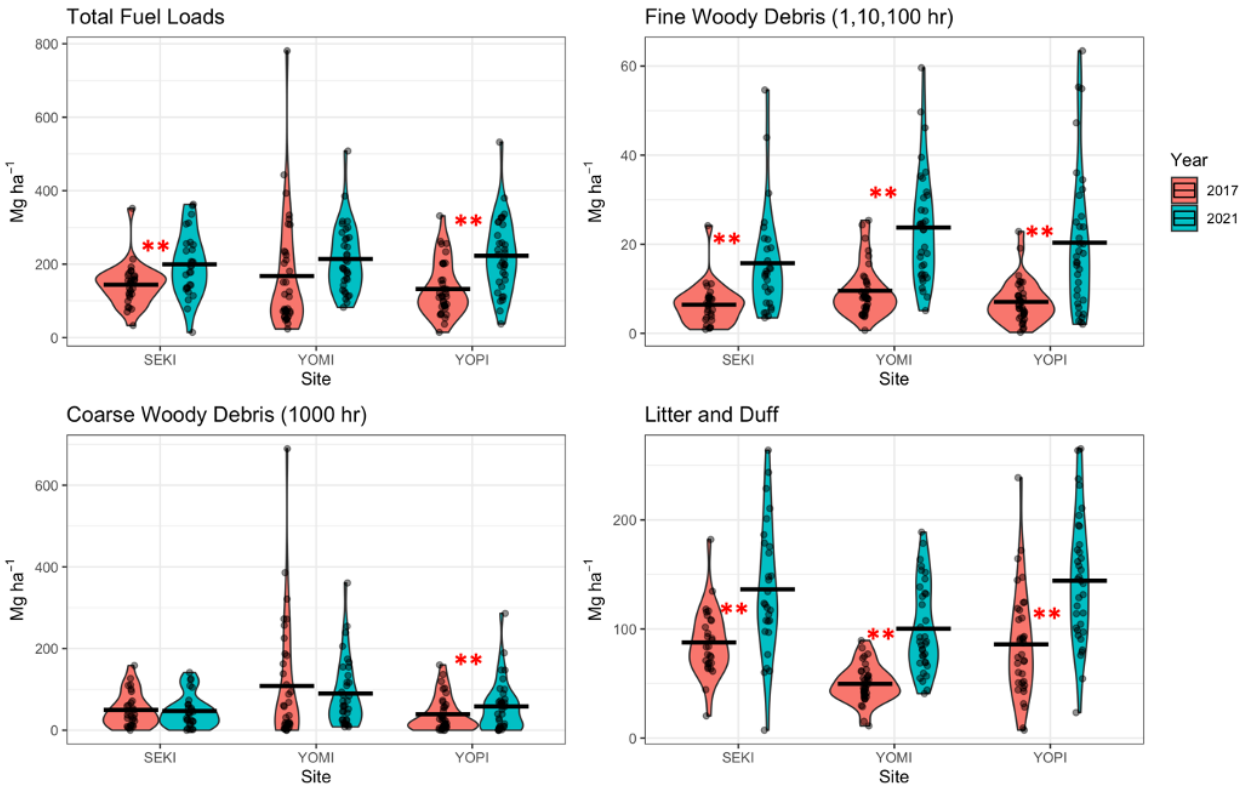

Figure 1. Violin plots of the fuel load estimates within each stratum at SEKI, YOMI, and YOPI measured in 2017 (red) and 2021 (blue). Horizontal lines represent mean fuel loads for given site and year. The colored region around each violin plot illustrates the proportion of data located at that given value and the dots represent actual measurements for a given plot. Groups of plots marked by ** denote a significant change from 2017 to 2021.

3.2 Snag Fall Rates

The USGS dataset observed 3,059 snags and 1,187 snag falls. Of the remaining 1,872 snags, 372 were right-censored due to fire and 1,500 did not fall during the observation period (Table 1). DBH of snags ranged from 12.7 to 251 cm. Diameter distributions for each species followed the general reverse J-shaped curve (Supplementary Figure S1).

Species	Number of snags	Number of snags that fell	Median Survival Time (25^{th} – 75^{th} percentile) (Years)	Mean DBH (cm) (Range)
White fir	1418	604	13 (8-26)	43 (12.7-162)
Red fir	412	147	17(9-27)	49.4 (12.7 – 251)
Incense-cedar	412	71	20 (13-UND)*	25.2 (12.7-184)
Sugar pine	483	211	13 (9-25)	41.1 (12.7-98.1)
Yellow pine	175	76	9 (6-16)	49.9 (12.7-162)
Black oak	159	78	14 (8-23)	23.6 (12.7-98.1)

304 **Table 1.** List of species included in the model, number of snags of each species, number of snags
305 that fell for each species, median survival time using Kaplan-Meier estimator, and mean DBH.
306 *75^{th} percentile is undefined due to skewedness of data.
307

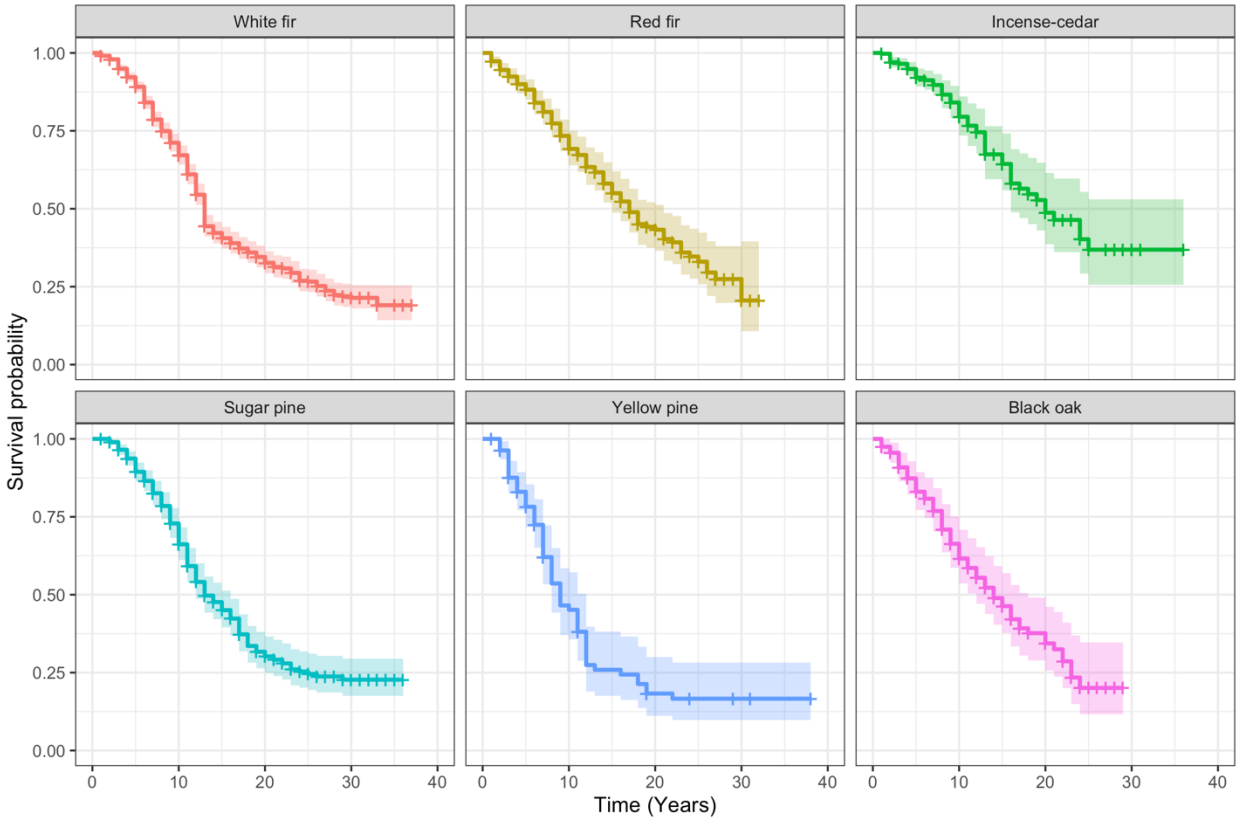

Figure 2. Observed survival curves using Kaplan-Meier estimator for each species with 95% confidence intervals (shaded areas). Curves depict survival probability of snags over time, by species.

Median survival times (Table 1) (Kaplan-Meir estimator), and the results from the log-rank test using species as groups ($\chi^2 = 47.8, df = 5, p < 0.01$) indicate that snag fall rates vary by species. Yellow pine snags had the shortest survival time with a median of 9 years while incense-cedar had the longest survival time with a median of 20 years.

The best performing AFT model used a log-logistic distribution and included the interaction of species and diameter as covariates. This modeled yielded the lowest AIC score (Supplementary Table S4), demonstrated good model performance with a concordance statistic of 0.6951 (SE = 0.009) and revealed a strong fit to the data (Figure 3).

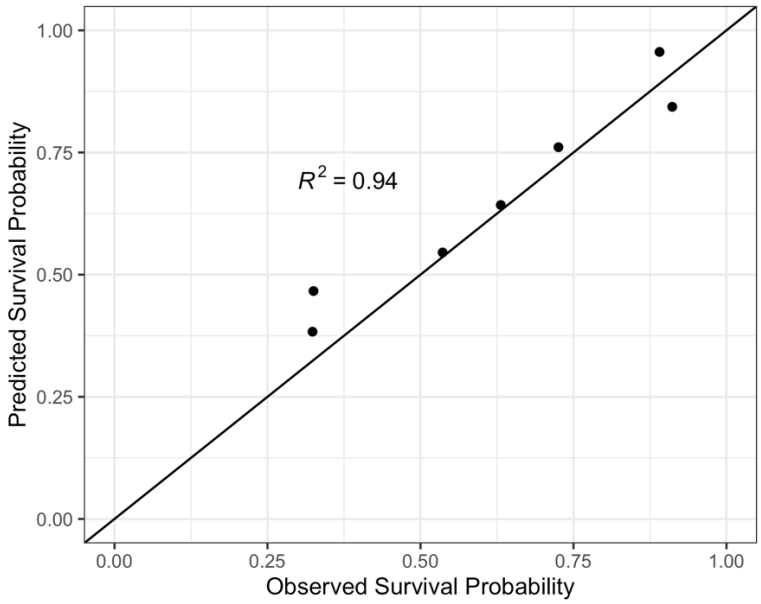

Figure 3. Average binned predicted survival probabilities calculated for all trees used to fit the top model (n = 3059), compared to actual proportion of trees that fell within a bin. Pseudo R^2 value reported on figure.

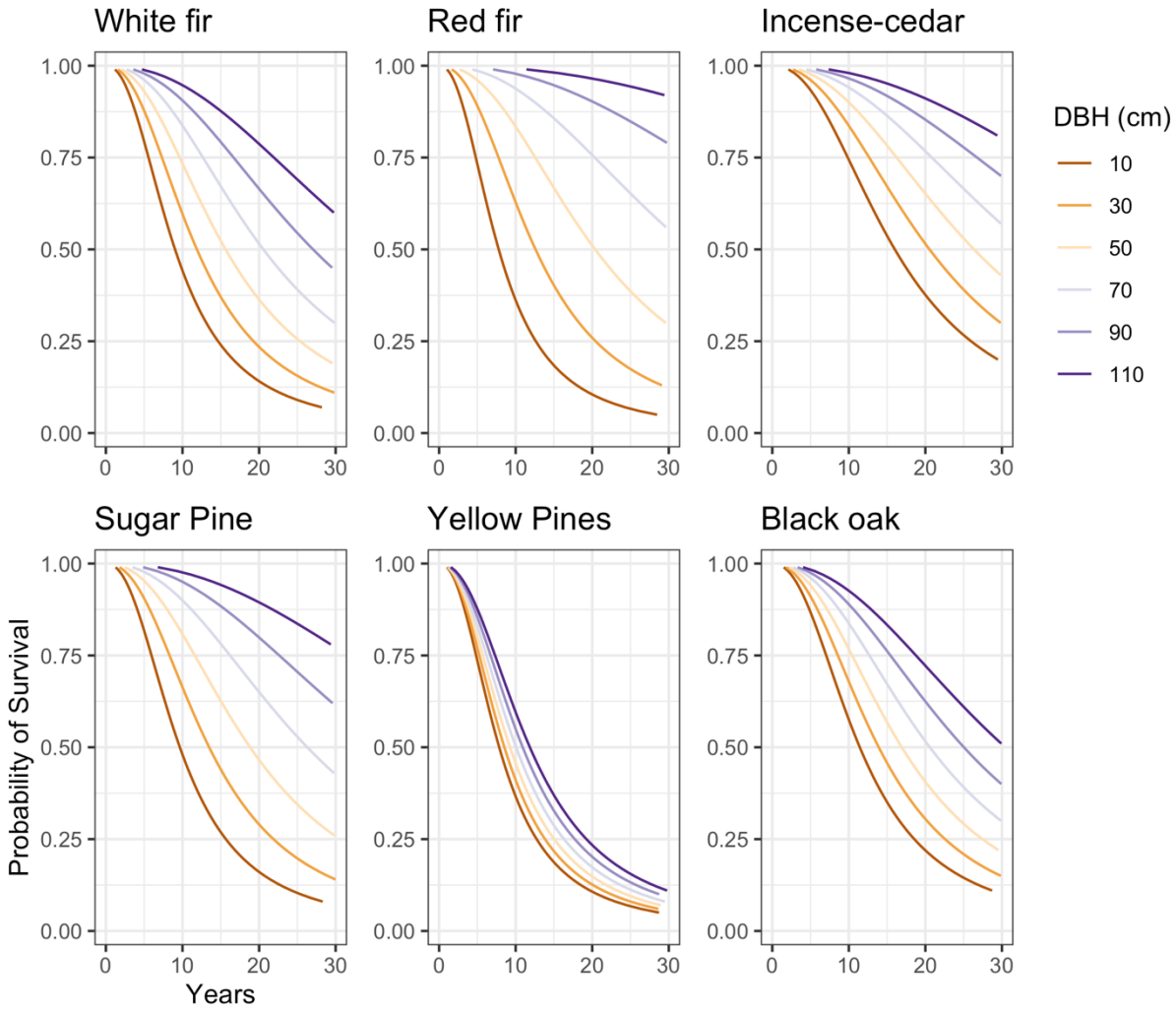

329

330 **Figure 4.** Predicted mixed conifer survival times for each species of different sizes.

331

332 Model results reveal a strong effect of both species and size and they highlight key
333 interactions between species and size (Figure 4, Supplementary Table S3 and Figure S2). Across
334 all species snag longevity increased with size, however, the effect varied by species. Size played
335 a small role in influencing yellow pine fall rates but a very large role in red fir and sugar pine
336 longevity. Size played an important, but less pronounced role for white fir, incense-cedar, and

337 black oak. When size is held constant, yellow pines fall the fastest while incense-cedars fall the
338 slowest.
339
340 *3.3 Snag Fall Rates and Fuel Loads*
341 Our projections suggest there will be large inputs of biomass from snag fall in the coming
342 decades in these Sierra Nevada mixed conifer forests. Based on 2017 field measurements, SEKI,
343 YOMI, and YOPI have an average of 162.4 (SE=31.07), 236.8 (64.05), and 165.08 (24.39) Mg
344 ha^{-1} of standing dead biomass in the form of snags, respectively. Our projections show that the
345 rate of input from snag fall varies across our three sites with YOPI having the fastest input of
346 snag material, with projections of 136.1 Mg ha^{-1} (115.6-150.6, 25^{th} and 75^{th} percentile values) of
347 biomass will fall by 2040 (Figure 5). YOMI is predicted to have a fast initial deposition of
348 material, with 92.3 Mg ha^{-1} (64.4-109.3) predicted to fall by 2040 followed by a slower but
349 steady input for the decades afterward (Figure 5). SEKI is projected to have the slowest biomass
350 deposition with 49.4 Mg ha^{-1} (30.9-80.3) predicted to fall by 2040, and the cumulative biomass
351 curve revealing a somewhat linear cumulative input over time (Figure 5).
352

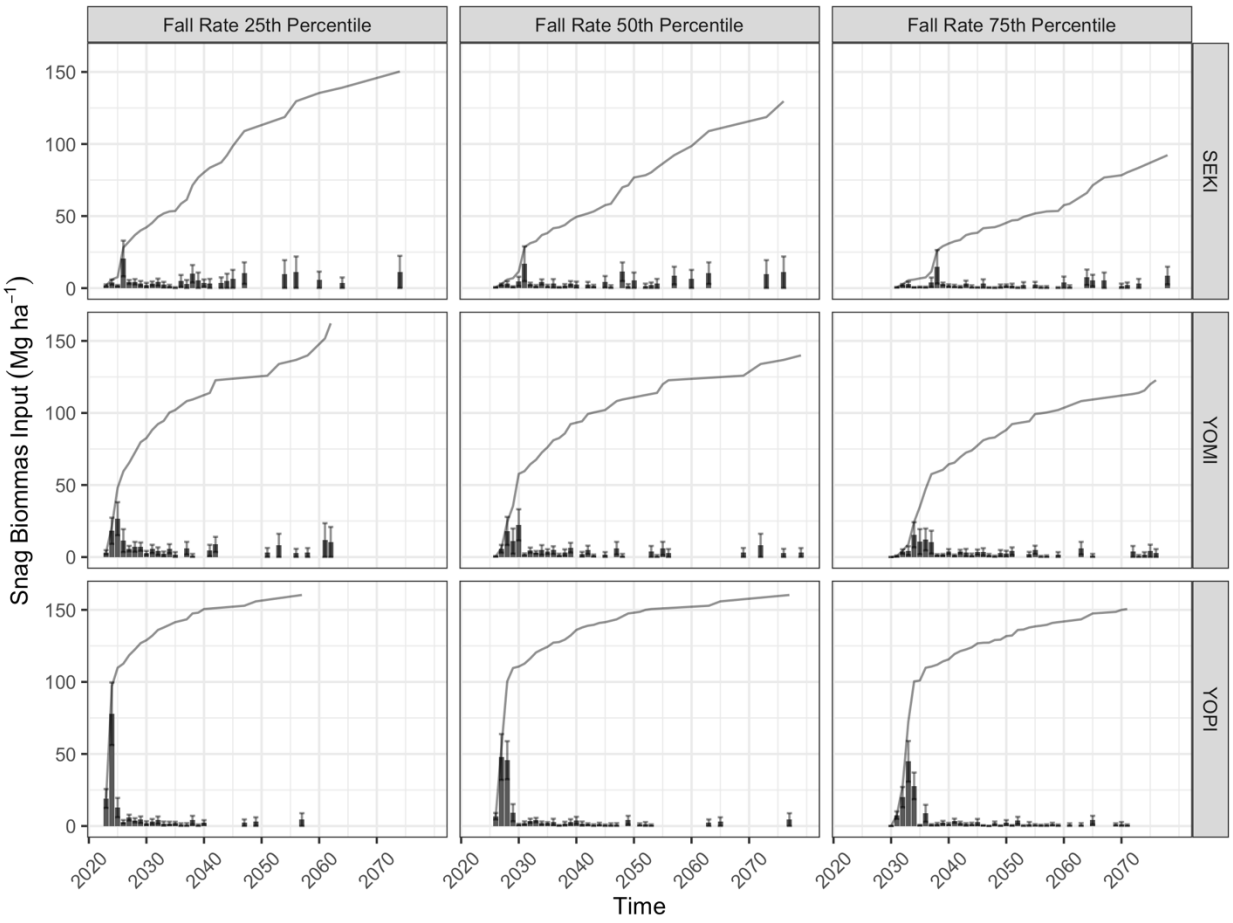

353

354 **Figure 5.** Forecasted biomass inputs over time based on current standing snags and model
355 predictions at SEKI, YOPI, and YOMI, based on 25th, 50th, and 75th percentile modeled fall rates.
356 Bars depict forecasted annual biomass input from snag fall, the error bars depict standard error of
357 annual biomass input, and the lines depict cumulative biomass input from snag fall.

358

359 **4. Discussion**

360 *4.1 Short- term changes in fuel loads*

361 Across all 3 sites we measured a significant increase in the amount of fine woody
362 material and litter and duff from 2017-2021. These results align well with theoretical timelines of
363 fuel loads following bark beetle mortality (Hicke et al., 2012; Stephens et al., 2018) as well as

empirical observations of fuel loads following similar mortality events in Rocky mountain lodgepole pine (*Pinus contorta* var. *latifolia* Englem. Ex Wats) forests (Klutsch et al., 2009; Page & Jenkins, 2007; Schoennagel et al., 2012), all of which propose or observe heightened fine woody material and litter loads as recently killed trees quickly lose leaves and fine twigs. Raphael and Morrison (1987) found that pine and fir snags in the Sierra Nevada lost most of their foliage and small branches within 5 years of mortality which suggests that the decay of snags created by the 2012-2016 drought are likely the primary source of the increases we observed.

There was only a significant increase in coarse woody debris loads at the YOPI site whose overstory is predominantly ponderosa pine (Supplementary Table S1). This confirms the implications from our fall rate model (Figure 4) and fuel projections (Figure 5) which show faster fall rates in yellow pines and the fastest input of biomass from snag fall at the YOPI site.

4.2 Snag fall rates

Our observed fall rates generally align with what has been reported in the past regarding mixed conifer species. Many studies report that ponderosa pine snags fall faster than fir snags and that incense-cedar snags often fall at the slowest rates (Grayson et al., 2022; Raphael & Morrison, 1987; Ritchie et al., 2013) which is consistent with our findings. While our observation that snag longevity increases with DBH is also common (Keen, 1955; Parish et al., 2010), an interactive effect between species and size has not been reported. Larger trees tend to have a greater volume of rot-resistant heartwood which provides structural support to standing trees (Harmon et al., 1986), and would explain the general trend that larger snags remain standing longer relative to smaller snags. The interaction of size and species is likely driven by

varying amounts of sapwood and heartwood within each species and the processes by which each species decays. Yellow pines trees decay much more rapidly than other species (Raphael & Morrison, 1987) so perhaps size is less important for these species since extra stability-providing heartwood simply degrades quickly, meaning larger trees only provide marginally more stability and snag survival time, as suggested in Figure 4. Ultimately, snag failure is most often a result of decay that has removed structural stability. The most common agents of wood decay are insects and fungi which often have species-specific interactions with snags (California Forest Insect and Disease Training Manual, 2006). Furthermore, rate of bark loss, aspect, and elevation also play a large role in decay (Audley et al., 2021; Harmon et al., 1986; Kimmey, 1955) so variation in those qualities likely contributed to the observed differences in the effects of species and size on fall rates.

4.3 Projection Long Term Changes in Fuel Loads

Our 3 study sites are projected to have large inputs of coarse woody material in the coming years as a result of the 2012-2016 drought (Figure 5). The YOPI site is projected to have the fastest inputs which is driven by the fast fall rates of yellow pine snags, whereas the SEKI and YOMI sites have more gradual inputs over time, likely due to a more mixed snag composition that yields varying and longer snag survival times. Regions of the Sierra Nevada that contain high densities of yellow pine snags will likely see rapid fall rates and heavy coarse woody material surface fuels more quickly similar to our projections for YOPI. On the contrary, regions with more balanced or less pine dominated snag compositions may see more gradual deposition of snag material, similar to YOMI and SEKI.

4.4 Model and Projection Limitations

There are a few assumptions and limitations to our modeling and projections that warrant discussion. A key assumption is that we assumed trees dead in 2017 would contain the same amount of biomass by the time of their predicted fall date. In reality, these trees will have decayed and lost some of their biomass over time, as reported in Cousins et al. (2015), implying that the actual biomass inputs from snags may be lower than those reported here. Our forecast also only considers snags present in 2017, and therefore omits fuel added from trees that die in the future.

Our model and projections also overlook other factors that are known to influence snag fall rates, so extrapolating our projections to other regions should be done with caution. For instance steeper slopes, moist soils, and southern aspects are known to increase fall rates while higher elevations, northern aspects, and higher canopy cover have been associated with lower fall rates (Audley et al., 2021; Keen, 1955; Rhoades et al., 2020; Ritchie et al., 2013). Since there is certainly variability in these conditions, it follows that the magnitude and timing of biomass inputs may vary from our predictions. Nonetheless, our results still highlight that a large amount of biomass is expected to be input to the surface within the next 20 years in the Sierra Nevada.

Snag persistence is a difficult process to model because there are many stochastic processes that can dramatically alter fall rates that are difficult to capture and include in a predictive model. Despite these difficulties, our top model revealed good performance (Figure 3) and had a high concordance statistic of 0.6951 which is higher than values reported in other snag fall rate model studies (Audley et al., 2021), and is within the range of values reported in Das et al. (2021). We emphasize that the large sample size (n=3059), annual resolution, and long temporal extent (up to 39 years) of our data contributed to the performance of our model.

4.5 Management Implications and Conclusion

Within our study sites and likely across a great deal of the western Sierra Nevada that experienced drought-related mortality, fine fuel loads have already increased, and coarse woody debris loads will rise in the coming 10-20 years as many snags fall to the ground. This increase in fuel loads from snag-fall, coupled with already heavy surface fuel loads, will increase the risk of high severity fire and potential for mass fire (Arno, 2000; Brown et al., 2003; Coppoletta et al., 2016; Stephens et al., 2018). There will be increased difficulties for wildland firefighting operations as snags falling represent a considerable danger to field crews and downed snags can hinder fireline construction and block vehicle access (Dunn et al., 2019; Plucinski, 2019). Managers should anticipate particularly fast fall rates and high coarse woody debris loads in areas containing high densities of large yellow pine snags, which were one of the most common targets of the recent bark beetle and drought mortality (Axelson et al., 2019; Fettig et al., 2019; Pile et al., 2019). We also highlight that the surface fuel loads we observed in 2017 prior to increases associated with the drought mortality were much greater than estimated historical loads in the Sierra Nevada or reported in the Sierra San Pedro Martir, a contemporary reference forest that never experienced logging or extensive fire suppression until the 1980s (Safford & Stevens, 2017; Stephens, 2004; Stephens et al., 2007).

Managers are not without options for dealing with the heightened surface fuels and large ground combustible biomass associated with extreme snag densities. Salvage logging operations could recover some of the economic value in the snags while also removing some of the snag biomass to lower future fuel input from snags (Prestemon et al., 2006). This is sometimes limited due to the rapid decline in timber value following tree mortality and the large amount of area inaccessible to logging operations in the Sierra Nevada due to factors such as protected habitats

and rugged topography, particularly on federally-owned land (North et al., 2015). Salvage operations may still be an option for some areas given that much of the Sierra Nevada is privately-owned and subject to fewer habitat restrictions (Stewart et al., 2016). Although expensive, non-economic salvage operations could also be conducted such as falling, piling, and burning snags to reduce snag biomass and future fuel inputs of coarse woody debris. While salvage operations can lower future inputs of fuel from snag fall, they cannot reduce surface fuels already present on the ground which is a key characteristic of successful forest restoration (Stephens et al., 2020).

To address this concern managers may consider using prescribed burning in areas of high mortality to consume recently deposited fine fuels from mortality and any coarse woody debris already present from snag fall (Knapp et al., 2005; Stephens et al., 2018). Our results suggest most snags will fall within the next 10-20 years (Figure 5). Since operating in areas of high snag densities can be dangerous it would be best to burn within the next few years before the period of frequent snag fall or to burn after most snags have fallen in 20 or more years to avoid burning under high-risk snag situations. It may be best to burn prior to snag fall to remove the high surface fuel loads already on the ground so that future coarse woody debris from snag fall is not embedded within already heightened surface fuels that increase risk of mass fires (Stephens et al., 2018). Burning is also likely to change the rate of snag fall and fuel input since snags exposed to fire often experience heightened fall rates afterward (Landram et al., 2002). Managers may be able to reduce fuels most-efficiently by burning prior to the snag fall and then reburning 10-20 years later after most snags have fallen to consume recently downed material as well. It is important to acknowledge the uncertainty surrounding these treatment options given that our projections do not incorporate the influence of fire on snag fall rates, burn operations may be

difficult in stands with high log densities, and coarse woody debris consumption may be limited under prescribed burning conditions (Knapp et al., 2005). Despite this uncertainty and the many regulatory, operational, and political barriers to implementing prescribed burning (Miller et al., 2020; York et al., 2020) it will remain a valuable tool for managers to consume the large amounts of combustible material associated with the 2012-2016 drought mortality event.

For forest managers, understanding the longevity of snags is crucial for future planning and decision-making, regarding minimizing risk for recreation and firefighter access to forests. A common tool used by managers to approach this issue is the Fire and Fuels Extension of the Forest Vegetation Simulator (FVS) which includes submodels that describe snag dynamics (Reinhardt & Crookston, 2003). Recent work by Grayson et al. (2019) suggests that FVS inaccurately predicts postfire snag fall rates and needs revision. We performed a comparison of predicted survival times using FVS, equations reported by Grayson et al. (2019), and our top performing model. Our comparison revealed strong difference in predictions with Grayson et al. (2019) reporting faster fall rates and FVS predicting slower fall rates (Table 2). We believe this highlights not only the importance of revising fall equations used in FVS but also the importance in using different fall rate equations based on the cause of death for snags since strong difference in fall rates for fire-killed versus non fire-killed snags have been reported (Grayson et al., 2019, this work).

Prediction Tool	Median predicted survival time (years)	Number of snags predicted to fall within 10 years	Number of snags predicted to fall within 20 years
Our top model	12.6	238	664
Grayson et al. 2019 equations	10.31	307	655
Forest Vegetation Simulator	14.75	0	556

Table 2. Comparison of predicted snag fall rates for snags from 2017 dead tree survey (771 snags), using our top model, equations reported in Grayson et al. (2019) and using predictions from the Forest Vegetation Simulator tool (Reinhardt & Crookston, 2003).

There are many difficulties and risks associated with managing forests following extensive mortality and providing managers with better tools and information to predict and anticipate snag fall rates will help address some of these challenges. This study provides managers with some essential information regarding snag longevity and fuel load accumulation following the extensive drought in the Sierra Nevada that can aid in future decision making.

References

Andersen, P. K., & Keiding, N. (2014). Survival Analysis, Overview. In N. Balakrishnan, T. Colton, B. Everitt, W. Piegorsch, F. Ruggeri, & J. L. Teugels (Eds.), *Wiley StatsRef: Statistics Reference Online* (1st ed.). Wiley. https://doi.org/10.1002/9781118445112.stat06060

Arno, A., S. F. (2000). Fire in western forest ecosystems. In *Wildland fire in ecosystems: Effects of fire on flora* (pp. 97–120).

Audley, J. P., Fettig, C. J., Steven Munson, A., Runyon, J. B., Mortenson, L. A., Steed, B. E., Gibson, K. E., Jørgensen, C. L., McKelvey, S. R., McMillin, J. D., & Negrón, J. F.

(2021). Dynamics of beetle-killed snags following mountain pine beetle outbreaks in lodgepole pine forests. *Forest Ecology and Management*, *482*, 118870. https://doi.org/10.1016/j.foreco.2020.118870

Axelson, J., Battles, J., Bulaon, B., Cluck, D., Cousins, S., Cox, L., Estes, B., Fettig, C., Hefty, A., Hishinuma, S., Hood, S., Kocher, S., McMahon, D., Mortenson, L., Koltunov, A., Kuskulis, E., Poloni, A., Ramirez, C., Restaino, C., … Young, D. (2019). The California Tree Mortality Data Collection Network—Enhanced communication and collaboration among scientists and stakeholders. *California Agriculture*, *73*(2), 55–62. https://doi.org/10.3733/ca.2019a0001

Barrows, J.S., 1951. Fire behavior in northern Rocky Mountain forests. Station Paper #29, USDA Forest Service, Northern Rocky Mountain Forest and Range Experiment Station, Missoula, MT.

Battles, John J., Cousins, Stella J.M., & Sanders, John E. (2015). *Carbon Dynamics and Greenhouse Gas Emissions of Standing Dead Trees in California Mixed Conifer Forests*. California Energy Commission.

Brown, J. K. (1974). *Handbook for Inventorying Downed Woody Material*. Forest Service Gen. Tech. Report INT-16. Ogden, Utah.

Brown, J. K., Reinhardt, E. D., & Kramer, K. A. (2003). *Coarse woody debris: Managing benefits and fire hazard in the recovering forest* (RMRS-GTR-105; p. RMRS-GTR-105). U.S. Department of Agriculture, Forest Service, Rocky Mountain Research Station. https://doi.org/10.2737/RMRS-GTR-105

California Forest Insect and Disease Training Manual. (2006). USDA.

Caprio, A., & Swetnam, T. (1993). *Historical Fire Regimes Along an Elevational Gradient on the West Slope of the Sierra Nevada, California*. Proceedings: Symposium on Fire in Wilderness and Park Management, General Technical Report INT-GTR-320 MIssoula, MT: USDA Forest Service.

Collins, B. J., Rhoades, C. C., Battaglia, M. A., & Hubbard, R. M. (2012). The effects of bark beetle outbreaks on forest development, fuel loads and potential fire behavior in salvage logged and untreated lodgepole pine forests. *Forest Ecology and Management*, *284*, 260–268. https://doi.org/10.1016/j.foreco.2012.07.027

Collins, B. M., Everett, R. G., & Stephens, S. L. (2011). Impacts of fire exclusion and recent managed fire on forest structure in old growth Sierra Nevada mixed-conifer forests. *Ecosphere*, *2*(4), art51. https://doi.org/10.1890/ES11-00026.1

Coppoletta, M., Merriam, K. E., & Collins, B. M. (2016). Post-fire vegetation and fuel development influences fire severity patterns in reburns. *Ecological Applications*, *26*(3), 686–699. https://doi.org/10.1890/15-0225

Cousins, S. J. M., Battles, J. J., Sanders, J. E., & York, R. A. (2015). Decay patterns and carbon density of standing dead trees in California mixed conifer forests. *Forest Ecology and Management*, *353*, 136–147. https://doi.org/10.1016/j.foreco.2015.05.030

Das, A. J., Slaton, M. R., Mallory, J., Asner, G. P., Martin, R. E., & Hardwick, P. (2022). Empirically validated drought vulnerability mapping in the mixed conifer forests of the SIERRA NEVADA. *Ecological Applications*, *32*(2). https://doi.org/10.1002/eap.2514

Diffenbaugh, N. S., Swain, D. L., & Touma, D. (2015). Anthropogenic warming has increased drought risk in California. *Proceedings of the National Academy of Sciences*, *112*(13), 3931–3936. https://doi.org/10.1073/pnas.1422385112

565 Dunn, C. J., O'Connor, C. D., Reilly, M. J., Calkin, D. E., & Thompson, M. P. (2019). Spatial
566 and temporal assessment of responder exposure to snag hazards in post-fire
567 environments. *Forest Ecology and Management*, *441*, 202–214.
568 https://doi.org/10.1016/j.foreco.2019.03.035
569 Fettig, C. J., Mortenson, L. A., Bulaon, B. M., & Foulk, P. B. (2019). Tree mortality following
570 drought in the central and southern Sierra Nevada, California, U.S. *Forest Ecology and*
571 *Management*, *432*, 164–178. https://doi.org/10.1016/j.foreco.2018.09.006
572 *Forest Inventory and Analysis National Core Field Guide Volume 1: Field Data Collection*
573 *Procedures for Phase 2 Plots, Version 5.0*. (2010). United States Department of
574 Agriculture, Forest Service (USFS).
575 Foster, D., Stephens, S.L., Moghaddas, J., Van Wagtendonk, J.,. 2018. Rfuels: Forest Fuels from
576 Brown's Transects. Berkeley, CA. https://github.com/danfosterfire/Rfuels.
577 Grayson, L. M., Cluck, D. R., & Hood, S. M. (2022). Correction to persistence of fire-killed
578 conifer snags in California, USA. *Fire Ecology*, *18*(1), 2. https://doi.org/10.1186/s42408-
579 021-00124-1
580 Griffin, D., & Anchukaitis, K. J. (2014). How unusual is the 2012-2014 California drought?:
581 GRIFFIN AND ANCHUKAITIS. *Geophysical Research Letters*, *41*(24), 9017–9023.
582 https://doi.org/10.1002/2014GL062433
583 Harmon, M. E., Franklin, J. F., Swanson, F. J., Sollins, P., Gregory, S. V., Lattin, J. D.,
584 Anderson, N. H., Cline, S. P., Aumen, N. G., Sedell, J. R., Lienkaemper, G. W.,
585 Cromack, K., & Cummins, K. W. (1986). Ecology of Coarse Woody Debris in Temperate
586 Ecosystems. In *Advances in Ecological Research* (Vol. 15, pp. 133–302). Elsevier.
587 https://doi.org/10.1016/S0065-2504(08)60121-X

588 Hicke, J. A., Johnson, M. C., Hayes, J. L., & Preisler, H. K. (2012). Effects of bark beetle-caused
589 tree mortality on wildfire. *Forest Ecology and Management*, *271*, 81–90.
590 https://doi.org/10.1016/j.foreco.2012.02.005
591 Hood, S. M., Smith, S. L., & Cluck, D. R. (2010). Predicting mortality for five California
592 conifers following wildfire. *Forest Ecology and Management*, *260*(5), 750–762.
593 https://doi.org/10.1016/j.foreco.2010.05.033
594 Jaffe, M. R., Collins, B. M., Levine, J., Northrop, H., Malandra, F., Krofcheck, D., Hurteau, M.
595 D., Stephens, S. L., & North, M. (2021). Prescribed fire shrub consumption in a Sierra
596 Nevada mixed-conifer forest. *Canadian Journal of Forest Research*, *51*(11), 1718–1725.
597 https://doi.org/10.1139/cjfr-2020-0454
598 James, I. (2014). Accelerated Failure-time Models. In N. Balakrishnan, T. Colton, B. Everitt, W.
599 Piegorsch, F. Ruggeri, & J. L. Teugels (Eds.), *Wiley StatsRef: Statistics Reference Online*
600 (1st ed.). Wiley. https://doi.org/10.1002/9781118445112.stat06002
601 Kaplan, E. L., & Meier, P. (1958). Nonparametric Estimation from Incomplete Observations.
602 *Journal of the American Statistical Association*, *53*(282), 457–481.
603 https://doi.org/10.1080/01621459.1958.10501452
604 Keen, F. P. (1955). The Rate of Natural Falling of Beetle-Killed Ponderosa Pine Snags. *Journal*
605 *of Forestry*, *53*(10), 720–723.
606 Kimmey, J. W. (1955). *Rate of Deterioration of fire-killed timber in California* (Vol. 962).
607 California Forest and Range Experiment Station.
608 Klutsch, J. G., Negrón, J. F., Costello, S. L., Rhoades, C. C., West, D. R., Popp, J., & Caissie, R.
609 (2009). Stand characteristics and downed woody debris accumulations associated with a

mountain pine beetle (Dendroctonus ponderosae Hopkins) outbreak in Colorado. *Forest Ecology and Management*, *258*(5), 641–649. https://doi.org/10.1016/j.foreco.2009.04.034

Knapp, E. E. (2015). Long-term dead wood changes in a Sierra Nevada mixed conifer forest: Habitat and fire hazard implications. *Forest Ecology and Management*, *339*, 87–95. https://doi.org/10.1016/j.foreco.2014.12.008

Knapp, E. E., Keeley, J. E., Ballenger, E. A., & Brennan, T. J. (2005). Fuel reduction and coarse woody debris dynamics with early season and late season prescribed fire in a Sierra Nevada mixed conifer forest. *Forest Ecology and Management*, *208*(1–3), 383–397. https://doi.org/10.1016/j.foreco.2005.01.016

Kolb, T. E., Fettig, C. J., Ayres, M. P., Bentz, B. J., Hicke, J. A., Mathiasen, R., Stewart, J. E., & Weed, A. S. (2016). Observed and anticipated impacts of drought on forest insects and diseases in the United States. *Forest Ecology and Management*, *380*, 321–334. https://doi.org/10.1016/j.foreco.2016.04.051

Landram, F.M., Laudenslayer Jr., W.F., Atzet, T., 2002. Demography of snags in eastside pine forests of California. In: Laudenslayer Jr., W.F., Shea, P.J., Valentine, B.V., Weatherspoon, C.P., Lisle, T.E. (Technical Coordinators), Proceedings of the Symposium on the Ecology and Management of Dead Wood in Western Forests. USDA For. Serv. Gen. Tech. Rep. PSW-181. Pacific Southwest Forest and Range Experimentation Station, Berkeley, CA, pp. 605–620.

Lydersen, J. M., Collins, B. M., Coppoletta, M., Jaffe, M. R., Northrop, H., & Stephens, S. L. (2019). Fuel dynamics and reburn severity following high-severity fire in a Sierra Nevada, USA, mixed-conifer forest. *Fire Ecology*, *15*(1), 43. https://doi.org/10.1186/s42408-019-0060-x

633 Lydersen, J. M., Collins, B. M., Knapp, E. E., Roller, G. B., & Stephens, S. (2015). Relating fuel
634 loads to overstorey structure and composition in a fire-excluded Sierra Nevada mixed
635 conifer forest. *International Journal of Wildland Fire*, *24*(4), 484.
636 https://doi.org/10.1071/WF13066
637 Miller, R. K., Field, C. B., & Mach, K. J. (2020). Barriers and enablers for prescribed burns for
638 wildfire management in California. *Nature Sustainability*, *3*(2), 101–109.
639 https://doi.org/10.1038/s41893-019-0451-7
640 Monsanto, P. G., & Agee, J. K. (2008). Long-term post-wildfire dynamics of coarse woody
641 debris after salvage logging and implications for soil heating in dry forests of the eastern
642 Cascades, Washington. *Forest Ecology and Management*, *255*(12), 3952–3961.
643 https://doi.org/10.1016/j.foreco.2008.03.048
644 Morrison, M. L., & Raphael, M. G. (1993). Modeling the Dynamics of Snags. *Ecological*
645 *Applications*, *3*(2), 322–330. https://doi.org/10.2307/1941835
646 North, M., Brough, A., Long, J., Collins, B., Bowden, P., Yasuda, D., Miller, J., & Sugihara, N.
647 (2015). Constraints on Mechanized Treatment Significantly Limit Mechanical Fuels
648 Reduction Extent in the Sierra Nevada. *Journal of Forestry*, *113*(1), 40–48.
649 https://doi.org/10.5849/jof.14-058
650 North, M. P., Tompkins, R. E., Bernal, A. A., Collins, B. M., Stephens, S. L., & York, R. A.
651 (2022). Operational resilience in western US frequent-fire forests. *Forest Ecology and*
652 *Management*, *507*, 120004. https://doi.org/10.1016/j.foreco.2021.120004
653 Page, Wesley G., & Jenkins, M. J. (2007). Mountain Pine Beetle-Induced Changes to Selected
654 Lodgepole Pine Fuel Complexes within the Intermountain Region. *Forest Science*, *53*(4),
655 507–518.

Parish, R., Antos, J. A., Ott, P. K., & Lucca, C. M. D. (2010). Snag longevity of Douglas-fir, western hemlock, and western redcedar from permanent sample plots in coastal British Columbia. *Forest Ecology and Management*, *259*(3), 633–640. https://doi.org/10.1016/j.foreco.2009.11.022

Pile, L., Meyer, M., Rojas, R., Roe, O., & Smith, M. (2019). Drought Impacts and Compounding Mortality on Forest Trees in the Southern Sierra Nevada. *Forests*, *10*(3), 237. https://doi.org/10.3390/f10030237

Plucinski, M. P. (2019). Contain and Control: Wildfire Suppression Effectiveness at Incidents and Across Landscapes. *Current Forestry Reports*, *5*(1), 20–40. https://doi.org/10.1007/s40725-019-00085-4

Preisler, H. K., Grulke, N. E., Heath, Z., & Smith, S. L. (2017). Analysis and out-year forecast of beetle, borer, and drought-induced tree mortality in California. *Forest Ecology and Management*, *399*, 166–178. https://doi.org/10.1016/j.foreco.2017.05.039

Prestemon, J. P., Wear, D. N., Stewart, F. J., & Holmes, T. P. (2006). Wildfire, timber salvage, and the economics of expediency. *Forest Policy and Economics*, *8*(3), 312–322. https://doi.org/10.1016/j.forpol.2004.07.003

R Core Team. 2019. *R: A Language and Environment for Statistical Computing*. Vienna, Austria: R Foundation for Statistical Computing. https://www.r-project.org/ (accessed June 1, 2022).

Raphael, M. G., & Morrison, M. L. (1987). Decay and Dynamics of snags in the Sierra Nevada, California. *Forest Science*, *33*(3), 774–783.

Raphael, M. G., & White, M. (1984). Use of Snags by Cavity-Nesting Birds in the Sierra Nevada. *Wildlife Monographs*, *86*, 3–66. JSTOR.

679 Reinhardt, E., & Crookston, N. L. (2003). *The Fire and Fuels Extension to the Forest Vegetation*
680 *Simulator* (RMRS-GTR-116; p. RMRS-GTR-116). U.S. Department of Agriculture,
681 Forest Service, Rocky Mountain Research Station. https://doi.org/10.2737/RMRS-GTR-
682 116
683 Rhoades, C. C., Hubbard, R. M., Hood, P. R., Starr, B. J., Tinker, D. B., & Elder, K. (2020).
684 Snagfall the first decade after severe bark beetle infestation of high-elevation forests in
685 Colorado, USA. *Ecological Applications*, *30*(3). https://doi.org/10.1002/eap.2059
686 Ritchie, M. W., Knapp, E. E., & Skinner, C. N. (2013). Snag longevity and surface fuel
687 accumulation following post-fire logging in a ponderosa pine dominated forest. *Forest*
688 *Ecology and Management*, *287*, 113–122. https://doi.org/10.1016/j.foreco.2012.09.001
689 Robeson, S. M. (2015). Revisiting the recent California drought as an extreme value.
690 *Geophysical Research Letters*, *42*(16), 6771–6779.
691 https://doi.org/10.1002/2015GL064593
692 Saab, V. A., Latif, Q. S., Rowland, M. M., Johnson, T. N., Chalfoun, A. D., Buskirk, S. W.,
693 Heyward, J. E., & Dresser, M. A. (2014). Ecological Consequences of Mountain Pine
694 Beetle Outbreaks for Wildlife in Western North American Forests. *Forest Science*, *60*(3),
695 539–559. https://doi.org/10.5849/forsci.13-022
696 Safford, H. D., & Stevens, J. T. (2017). *Natural range of variation for yellow pine and mixed-*
697 *conifer forests in the Sierra Nevada, southern Cascades, and Modoc and Inyo National*
698 *Forests, California, USA* (PSW-GTR-256; p. PSW-GTR-256). U.S. Department of
699 Agriculture, Forest Service, Pacific Southwest Research Station.
700 https://doi.org/10.2737/PSW-GTR-256

Schoennagel, T., Veblen, T. T., Negron, J. F., & Smith, J. M. (2012). Effects of Mountain Pine Beetle on Fuels and Expected Fire Behavior in Lodgepole Pine Forests, Colorado, USA. *PLoS ONE*, *7*(1), e30002. https://doi.org/10.1371/journal.pone.0030002

Stephens, S. L. (2004). Fuel loads, snag abundance, and snag recruitment in an unmanaged Jeffrey pine–mixed conifer forest in Northwestern Mexico. *Forest Ecology and Management*, *199*(1), 103–113. https://doi.org/10.1016/j.foreco.2004.04.017

Stephens, S. L., Battaglia, M. A., Churchill, D. J., Collins, B. M., Coppoletta, M., Hoffman, C. M., Lydersen, J. M., North, M. P., Parsons, R. A., Ritter, S. M., & Stevens, J. T. (2020). Forest Restoration and Fuels Reduction: Convergent or Divergent? *BioScience*, biaa134. https://doi.org/10.1093/biosci/biaa134

Stephens, S. L., Collins, B. M., Fettig, C. J., Finney, M. A., Hoffman, C. M., Knapp, E. E., North, M. P., Safford, H., & Wayman, R. B. (2018). Drought, Tree Mortality, and Wildfire in Forests Adapted to Frequent Fire. *BioScience*, *68*(2), 77–88. https://doi.org/10.1093/biosci/bix146

Stephens, S. L., & Finney, M. A. (2002). Prescribed fire mortality of Sierra Nevada mixed conifer tree species: Effects of crown damage and forest floor combustion. *Forest Ecology and Management*, *162*(2–3), 261–271. https://doi.org/10.1016/S0378-1127(01)00521-7

Stephens, S. L., Fry, D. L., Franco-Vizcaíno, E., Collins, B. M., & Moghaddas, J. M. (2007). Coarse woody debris and canopy cover in an old-growth Jeffrey pine-mixed conifer forest from the Sierra San Pedro Martir, Mexico. *Forest Ecology and Management*, *240*(1–3), 87–95. https://doi.org/10.1016/j.foreco.2006.12.012

Stephenson, N. L., Das, A. J., Ampersee, N. J., Bulaon, B. M., & Yee, J. L. (2019). Which trees die during drought? The key role of insect host-tree selection. *Journal of Ecology*, *107*(5), 2383–2401. https://doi.org/10.1111/1365-2745.13176

Stevens, D. L., & Olsen, A. R. (2003). Variance estimation for spatially balanced samples of environmental resources. *Environmetrics*, *14*(6), 593–610. https://doi.org/10.1002/env.606

Stewart, W., Sharma, B., York, R., Diller, L., Hamey, N., Powell, R., Swiers, R. (2016). Forestry. In Mooney, H. & Zavaleta, E. (Eds), *California Ecosystems* (pp, 817-834). University of California Press.

Therneau, T. M. 2015. "A Package for Survival Analysis in S." https://cran.r-project.org/package=survival (accessed Jan 1, 2022).

[USDA] United States Department of Agriculture. 2019. Survey Finds 18 Million Trees Died in California in 2018. Press release. Feb. 1, 2019. Number of Dead Trees in California 2010 to 2018 (all lands). https://www.fs.usda.gov/Internet/FSE_DOCUMENTS/fseprd609297.pdf (accessed Apr 14, 2022).

Whitlock, M., & Schluter, D. (2020). Survival Analysis. In *The Analysis of Biological Data* (3rd ed., pp. 687–710).

York, R. A., Roughton, A., Tompkins, R., & Kocher, S. (2020). Burn permits need to facilitate – not prevent – "good fire" in California. *California Agriculture*, 62–66. https://doi.org/10.3733/ca.2020a0014

Supplementary Materials

Site	Mean Live Density (SE) (trees ha^{-1})	Mean Dead Density (SE) (trees ha^{-1})	Mean Live Basal Area (SE) (m^2 ha^{-1})	Mean Dead Basal Area (SE) (m^2 ha^{-1})	Dominance (%)
SEKI	312.7 (33.4)	121.8 (22.2)	41.9 (4.8)	21.4(3.3)	White fir (32%) Incense-cedar (26%)
YOMI	201.5(17.3)	147.4 (17.9)	51.2 (5.9)	26.2 (5.0)	Incense-cedar (25%) White fir (20%)
YOPI	351.7 (32.8)	205.6 (31.9)	39.6 (6.4)	32.2 (5.4)	Ponderosa pine (55%) Incense-cedar (28%)

Supplementary Table S1. Overstory structure and composition from 2017 tree inventory at sites where fuel loads were measured. Dominance shows 2 most dominant tree species observed based on relative basal area percentages at each site.

Site	Fuel Strata	2017 (SE) Mg ha^{-1}	2021 (SE) Mg ha^{-1}	Mean Change (SE) Mg ha^{-1}	t-value	P-value
SEKI	**Total**	**143.83 (11.04)**	**199.26 (16.28)**	**55.43 (17.97)**	**3.0844**	**0.004667**
YOPI	**Total**	**132 (12.42)**	**222.84 (16.97)**	**90.69 (13.63)**	**6.6562**	**1.226e-07**
YOMI	Total	167.63 (26.16)	214.05 (15.48)	46.42 (30.42)	1.5261	0.1362
SEKI	**FWD**	**6.42 (0.88)**	**15.75 (2.25)**	**9.32 (2.26)**	**4.1275**	**0.0003156**
YOPI	**FWD**	**7.04 (0.82)**	**20.36 (2.69)**	**13.32 (2.48)**	**5.3742**	**5.609e-06**
YOMI	**FWD**	**9.57 (0.99)**	**23.73 (2.11)**	**14.17 (2.11)**	**6.7121**	**1.04e-07**
SEKI	CWD	49.64 (7.91)	47.17 (7.72)	-2.48 (10.16)	-0.24357	0.8094
YOPI	**CWD**	**39.21 (7.27)**	**58.17 (10.64)**	**18.96 (8.49)**	**2.2326**	**0.03227**
YOMI	CWD	108.26 (24.96)	89.97 (13.93)	-18.29 (27.42)	-0.66696	0.5093
SEKI	**Litter and Duff**	**87.77 (5.87)**	**136.35 (11.34)**	**48.54 (10.14)**	**4.7884**	**5.379e-05**
YOPI	**Litter and Duff**	**85.89 (8.27)**	**144.32 (9.76)**	**58.43 (7.49)**	**7.79**	**4.51e-09**
YOMI	**Litter and Duff**	**49.8 (2.94)**	**100.35 (6.85)**	**50.54 (7.74)**	**6.5266**	**1.798e-07**

Supplementary Table S2. Mean fuel loads in each fuel strata, at each site, in 2017 and 2021, mean change in fuel loads for each stratum, and result of paired t-test between years at SEKI, YOMI, and YOPI. Values in bold denote significant change at an alpha level of 0.05.

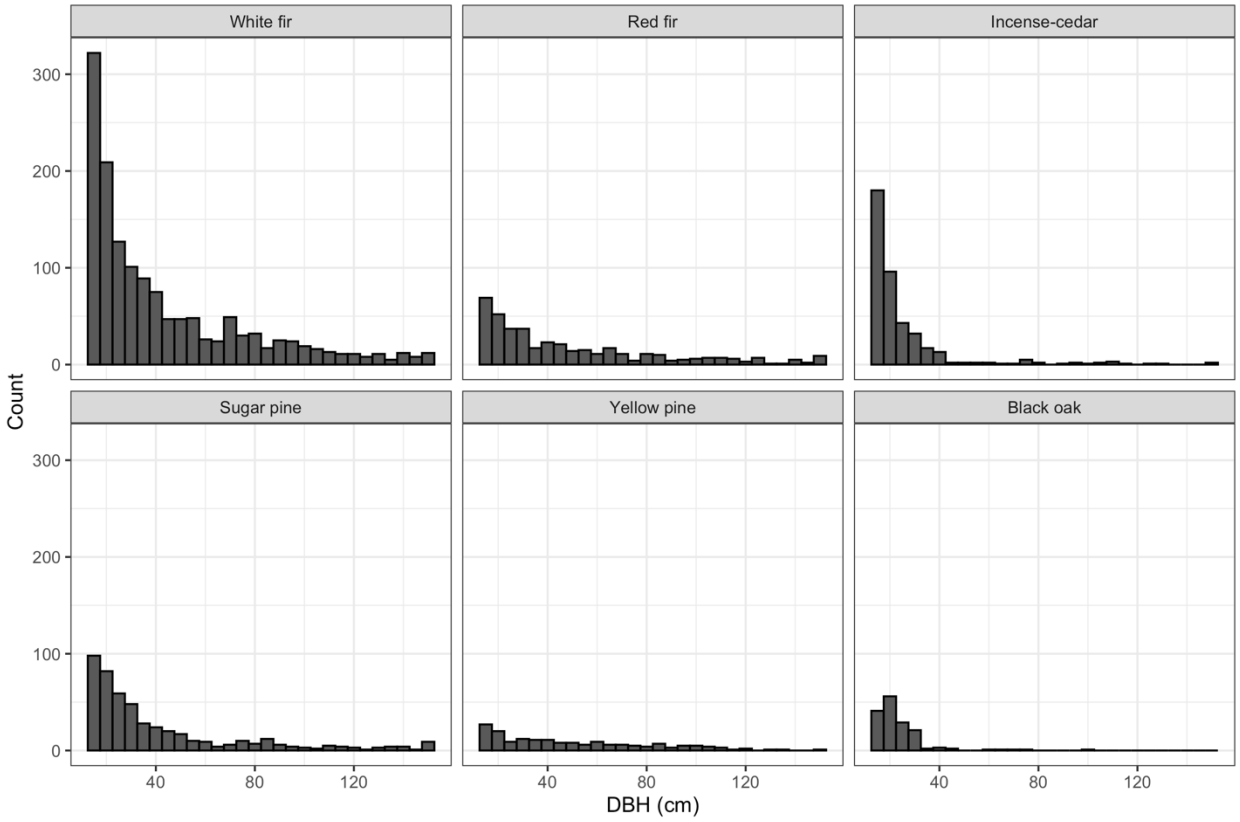

Supplementary Figure S1. Diameter distributions for each species included in our analysis of snag fall rates. All trees with a DBH greater than 150 cm were placed into a 150+cm bin to improve visual appearance of histograms. Yellow pine includes ponderosa pine and Jeffrey pine.

Covariate	Estimate	Standard Error	Z	P-value
Intercept	**2.06138**	**0.042679**	**48.34**	**<2e-16**
DBH	**0.013717**	**0.000943**	**14.55**	**<2e-16**
ABCO	Reference	na	na	na
ABMA	**-0.251443**	**0.114400**	**-2.20**	**0.02795**
CADE	**0.585106**	**0.165697**	**3.53**	**0.00041**
PILA	0.037314	0.090075	0.41	0.67869
PINE	-0.043574	0.141739	-0.31	0.75852
QUKE	0.275379	0.186104	1.48	0.13895
DBH*ABCO	Reference	na	na	na
DBH*ABMA	**0.010341**	**0.003049**	**3.39**	**0.00069**
DBH*CADE	-0.001248	0.007489	-0.17	0.86764
DBH*PILA	0.002984	0.002431	1.23	0.21956
DBH*PINE	**-0.009595**	**0.002550**	**-3.76**	**0.00017**
DBH*QUKE	-0.003921	0.007460	-0.53	0.59922
Log(scale)	**-0.819829**	**0.022814**	**-35.94**	**<2e-16**

Supplementary Table S3. Estimated parameters of the accelerated failure time model with lowest AIC predicting snag survival time. Values in bold denote significant change at an alpha level of 0.05.

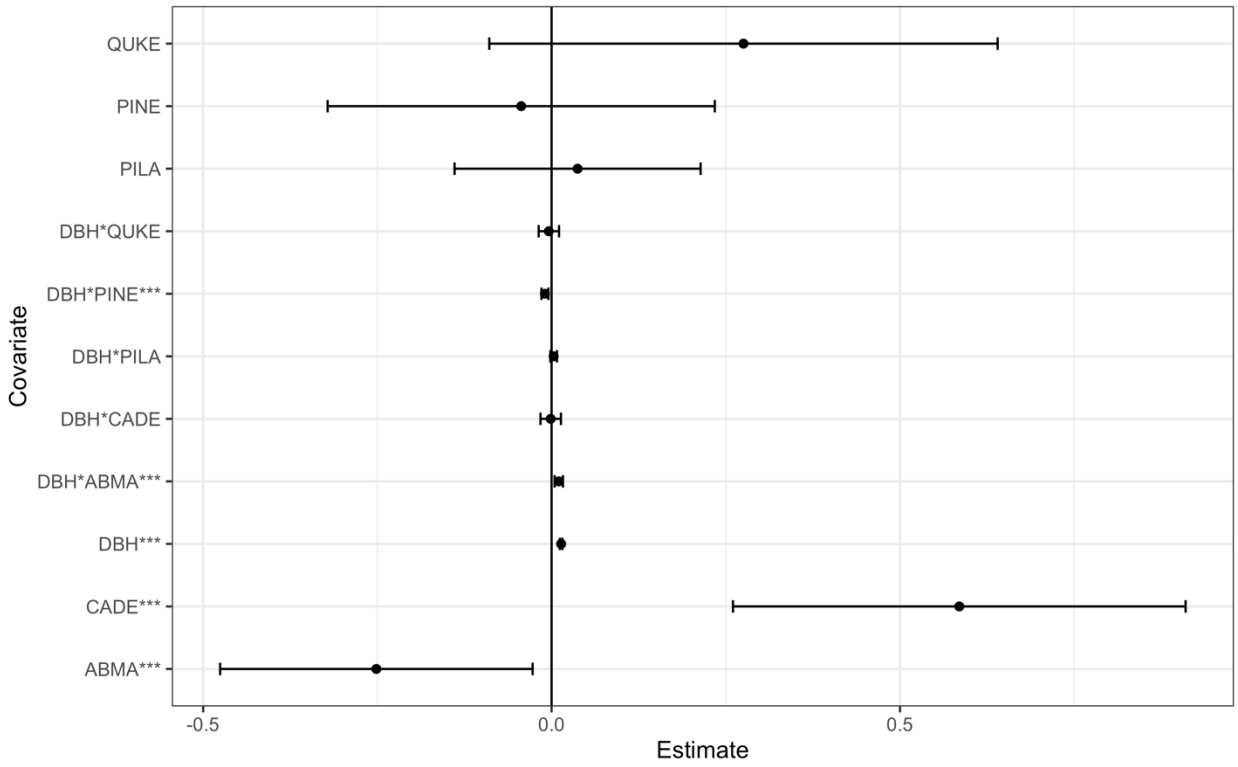

Supplementary Figure S3. Estimated parameters and 95% confidence intervals of the accelerated failure time model with lowest AIC predicting snag survival time. Parameter estimates that are significant at $\alpha = 0.05$ are labeled with ***

Model Covariates	AIC	ΔAIC	Concordance (SE)
DBH * Species	9046.007	0	0.6951 (0.008929)
DBH + Species	9068.152	22.145	0.6846 (0.008895)
DBH	9177.373	131.366	0.6541 (0.009063)
Species	9454.527	408.52	0.552 (0.009739)
Null	9493.797	447.79	0.5 (0)

Supplementary Table S4. Model covariates, AIC scores, and concordance statistics of all 5 log-logistic AFT models.